Investigating the Moisture Absorption Behavior of Bamboo Fiber-reinforced Epoxy Composites by Modelling

Yanping Zou,[a,b,d] Wenfu Zhang,[b,d,*] Hong Chen,[a] and Haitao Cheng [c]

The aim of this research was to investigate the moisture absorption of bamboo fibers (BFs) and their composites manufactured using different methods. The hygroscopic properties of BFs, jute fibers (JFs), glass fibers (GFs), and epoxy (EP) were compared and analyzed using dynamic vapor sorption (DVS), as well as the hygroscopic properties of the BF-Naval Ordnance Laboratory (BF-NOL), JF-NOL, GF-NOL, and bamboo fiber-reinforced epoxy composites manufactured *via* filament winding (FW), hot pressing (HP), and resin transfer molding (RTM). The results were analyzed using the Guggenheim-Anderson-deBoer (GAB), parallel exponential kinetics (PEK), and DoseResp models. The results indicated that BFs conformed to type II. The moisture adsorption isotherms of BF-NOL, JF-NOL, GF-NOL, and BF composites prepared by different molding processes exhibited a typical V-shape. The GAB and DoseResp models provided good fits to the changes in adsorption and desorption processes. The final equilibrium moisture content (EMC) of BFs and BF-NOL were 27.1% and 3.95%, respectively, the final EMC of BF composites prepared by RTM was 2.34%.

DOI: 10.15376/biores.18.1.272-290

Keywords: Bamboo fibers; Plant fibers; Moisture absorption; Dynamic vapor sorption (DVS)

*Contact information: a: College of Furnishings and Industrial Design, Nanjing Forestry University, Nanjing, 210037, China; b: Zhejiang Academy of Forestry, Hangzhou, 310023, China; c: International Center for Bamboo and Rattan, Beijing 100102, China; d: Key Laboratory of Bamboo Research of Zhejiang Province, Hangzhou, 310023, China *Corresponding author: zhangwenfu542697@163.com*

INTRODUCTION

Natural bamboo fiber, which is separated from bamboo, has been informally called "natural glass fiber" on account of its high specific strength and specific modulus (Wang *et al.* 2011; Khalil *et al.* 2012). The mechanical properties of bamboo fiber-reinforced composites (BFRCs) prepared from bamboo fibers (BFs) are comparable to those of glass fiber-reinforced composites (GFRCs). Compared with traditional fiber-reinforced composites (FRCs), BFRCs are cost-effective and environmentally friendly, and BFRCs can be widely applied in green packaging materials, automotive molded linings, machine product housings, and home decoration (Hao 2020). Epoxy (EP) is a thermosetting polymer synthetic material with good adhesion, corrosion resistance, insulation, and high strength (Sun 2002). The BFRCs prepared with EP as the matrix are environmentally friendly and strong, and have good fatigue resistance, thus they can replace GFRCs in some applications (Sun *et al.* 2011; Li 2016; Mittal *et al.* 2016; Saba *et al.* 2016). However, BF is a typical plant fiber. Hence, the surface of cellulose in bamboo fiber contains a large number of hydroxyl groups, which easily combine with water molecules to form hydrogen bonds

(Bledzki and Gassan 1999). Moisture has a detrimental effect on the composite performance, since it can reduce fiber properties and cause fiber swelling and fiber matrix debonding, leading to increased porosities and micro crack contents, all resulting in a decrease of the composite properties (Joseph *et al*. 2002; Dhakal *et al*. 2007; Newman 2009; Azwa *et al*. 2013; Le *et al*. 2015). The consequent problems arose in bamboo-based composites such as physical deforming, biodegradation, and weakness in strength will restrict its long-term use for applications under sever environmental conditions. Therefore, it is important to further study the hygroscopic properties of BFRCs.

The moisture sorption isotherm is often used to describe the relationship between the equilibrium moisture states of materials and their surrounding environment at constant temperature and relative humidity (RH), and this includes the adsorption isotherm measured from an initial dry condition and the desorption isotherm measured from an initially water-saturated condition (Yao 2018). Presently, the mathematical model describing the moisture changes could be obtained by non-linear fitting of the absorption and desorption processes of the material, providing a theoretical basis for the analysis of absorption properties of the material. Common moisture adsorption models include Guggenheim-Anderson-deBoer (GAB), BET, Halsey, Hendserson, Peleg, Smith, and Hailwood-Horrobin. These models are mainly used to analyze the relationship between equilibrium moisture content (EMC) and RH by fitting and analyzing the moisture absorption and desorption isotherms of materials, but different models have different applications. Among them, the GAB model is suitable for materials with large changes in RH, as it can better reflect the moisture absorption of materials. The BET model is suitable for hydrophilic materials when RH is < 50%, whereas the Halsey-Henderson semi-empirical model is suitable for food and agricultural products. The Peleg model is suitable for adsorbing S-type materials. The Smith model shows good fitting of the absorption of starch and cellulose materials, whereas the Hailwood-Horrobin model describes the absorption of materials but cannot describe the desorption of materials (Peng and Cai. 2018; Tamrakar and Lopez-Anido. 2011; Hill and Beck. 2017; Zelinka *et al.* 2018; Zhang *et al*. 2018). Furthermore, Kohler *et al.* (2003) proposed the parallel exponential dynamics model (PEK-model), which is used for the fast and slow adsorption of fiber-reinforced materials. It can also characterize the water adsorption characteristics of fiber bundles and wood under different RH and analyze the absorption and desorption processes of these materials (Kohler *et al.* 2006; Xie *et al.* 2011; Yao and Cai 2018).

The hygroscopic property of bamboo-based composites is mainly influenced by the bamboo species and chemical compositions (Zhang *et al*. 2018), resin types (Deka and Saikia 2000) as well as modification methods of the raw bamboo materials (Rahman 2018). The BFs were taken as the reinforcement and the EP was used as the matrix material in the BFRC. Besides, the BFRC had been subjected to different manufacturing processes. Hence, the hygroscopic property of the BFRC is expected to be differ from that of the raw bamboo. Nevertheless, the hygroscopic property of the BFRC has not been fully characterized and understood. Therefore, it is critical to investigate the performance of the dynamic moisture sorption for the BFRC, in order to estimate its industrial applications. To study the hygroscopic properties of BFRPs, the authors used the GAB and PEK models to compare and analyze the hygroscopic properties of different materials as well as bamboo fiber-reinforced epoxy composites, and used the DoseResp model to make prediction, hoping to provide theoretical support for the application of bamboo fiber composites.

EXPERIMENTAL

Materials

The BFs were homemade, 2- to 3-year-old *Neosinocalamus affinis* (*Bambusa emeiensis*) and were obtained from Sichuan Province, China. The bamboo culm at the height of more than 1.5 m from the base were cut and air-dried to moisture content of 8 to 12%. Bamboo sheets were turned into loose bundles of BFs by repeated grinding, then twisted into BFs with a bamboo fiber felting machine (homemade). After gathering the material into narrow fiber strips by means of a bamboo fiber directional narrowing machine (homemade), the bamboo fiber was processed into bamboo fiber yarn by bamboo fiber twisting machine (homemade).

JFs were purchased from a local market (Zhejiang Baisheng Industrial Co., Ltd., Zhejiang, China.) as a single strand yarn, GFs were also purchased from a local market as a coarse yarn (product grade, ECT550-1080). The GFs were free of alkalis and stranded into twist-free roving (made from multiple glass fiber strands). The moisture content was $\leqslant$ 0.10%, the bulk density was 1.65 g/cm^3, and the tensile strength was $\geqslant$ 0.35 N/Tex. The epoxy resin system, which consisted of epoxy resin (YD127) and solidification agent (EC201), was purchased from Nan Ya Electronic Materials (Kunshan) Co., Ltd. (China). The diameter information of raw materials is shown in Table 1.

Table 1. Diameters of raw materials

Index	Diameter (mm)
BFs	1.48
JFs	0.87
GFs	0.01

Preparation of Composites

A comparison chart of different processes is shown in Fig. 1. For the filament winding (FW), a Naval Ordnance Laboratory (NOL) ring, which is a circumferential winding fiber-reinforced sample, was fabricated according to the ASTM D2291-16 (2016) standard.

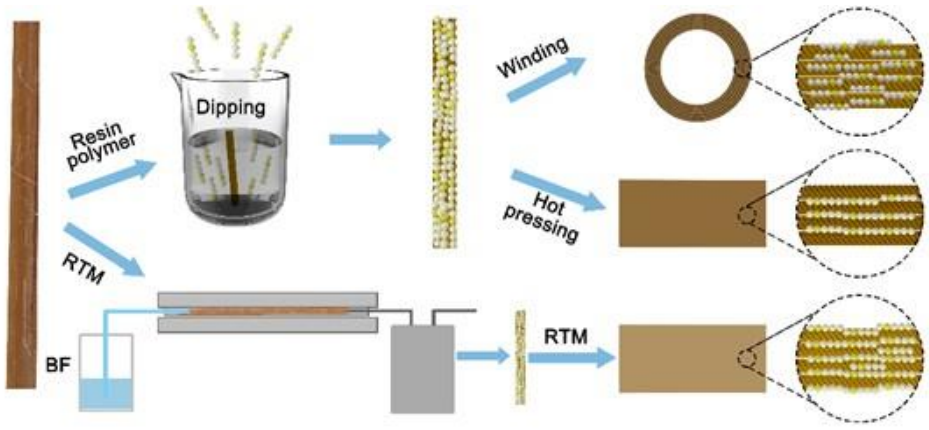

Fig. 1. Comparison chart of different processes

The hot pressing (HP) of the fiber composites was achieved using a hot-pressing machine (hot in, cold out) and a fixed-thickness frame mold with a thickness of 5 mm. The HP parameters involved a hot-pressing pressure of 2 MPa, a hot-pressing time of 2 min/mm, and a hot-pressing temperature equal to 120 °C. During the pressure release, the temperature of the hot-pressing machine was 50 °C. For the resin transfer molding (RTM), the bamboo fiber composites were fabricated using a vacuum adhesive injector with a vacuum level of 0.09 MPa, an injection pressure of 0.2 MPa, a solidification temperature of 120 °C, and a solidification rate of 2 min/mm.

Dynamic Water Vapor Sorption

The water vapor sorption behavior of samples was determined using a dynamic vapor sorption apparatus (DVS Resolution, Surface Measurement Systems Ltd., London, UK). The samples were placed on a holder connected to a microbalance (± 0.1 μg) using hanging wires, and this was located in a thermostatically controlled chamber where a constant flow of dry nitrogen gas into which another flow of nitrogen containing a preset amount of water vapor was mixed to maintain a given RH of 26%. The tests were taken at a constant temperature of 25 ± 0.1 °C, starting at 0% RH and increasing in increments of 10% RH up to 95% RH, then decreasing back to 0% RH also in 10% RH decrements. Samples were then maintained at a constant RH, and data on temperature, humidity, and weight change were collected every 0.6 s.

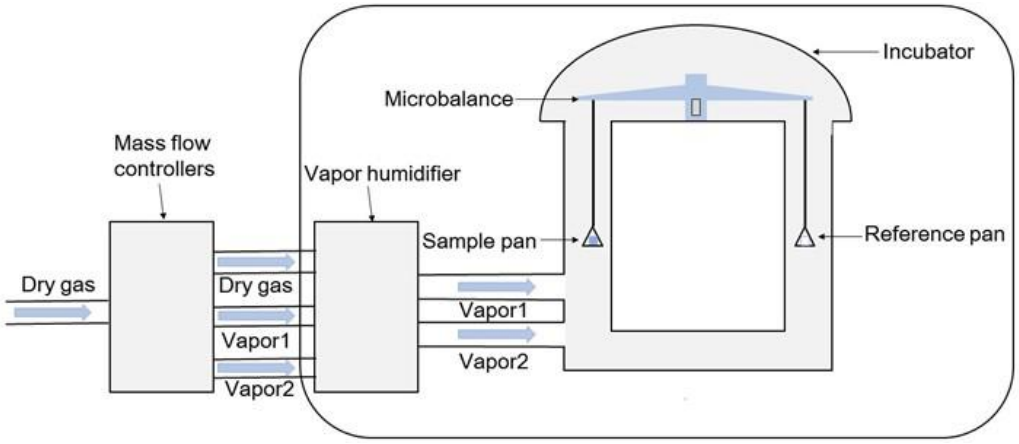

Fig. 2. A schematic for dynamic vapor sorption instrument

Sorption Models

Several mathematical models have been developed to describe the water vapor sorption isotherms of hygroscopic materials. The experimental sorption data of bamboo fibers and their composites prepared by FW, HP, and RTM were fitted with GAB and PEK models and predicted by DoseResp model (Table 2).

Table 2. Sorption Isotherm Models for Fitting and Predicting Experimental Data

Model Names	Model Equations
GAB model (Simpson 1980)	$EMC = \frac{W_0 C K a_w}{(1 - K a_w)(1 - K a_w + K C a_w)}$
PEK model (Kohler *et al.* 2003)	$MC = MC_0 + MC_1\left(1 - e^{\frac{t}{t_1}}\right) + MC_2\left(1 - e^{\frac{t}{t_2}}\right)$
DoseResp model (Self-created)	$\mathrm{EMC} = A_1 + \frac{A_2 - A_1}{(1 + 10^{(lgx_0 - a_w)\times P})}$

In Table 2, EMC is the EMC of samples (%), W_0 is the monolayer value (%), a_w is the water activity (a_w = equilibrium relative humidity (ERH)/ 100), MC is the moisture content (%) reached by the sample at any point of the moisture absorption or desorption at that stage, MC_0 is the initial moisture content of the sample (%), MC_1 and MC_2 are the moisture content (%) of the fast and slow processes, respectively, t is the arbitrary time (min), t_1 and t_2 are the time (min) of the fast and slow processes, respectively, and lgx_0 is the resin related to the initial variables.

The Origin 8.0 software (OriginLab Corporation, Northampton, MA, USA) was used for obtaining the parameters of the models.

RESULTS AND DISCUSSION

Hygroscopic Behavior on Raw Materials

Changes in moisture content and equilibrium time

The hygroscopic properties of BFs, JFs, GFs, and EP were determined, and the moisture adsorption kinetic curves of them were derived (Fig. 3). The EMC and the adsorption time at different RH were also analyzed (Table 3).

As shown in Fig. 3 and Table 3, the EMC increased in stages as the RH increased. At the highest RH (95%), BFs and JFs reached an EMC of 20.6% and 21.4%, respectively, whereas those of GFs and EP were 0.063% and 0.051%, respectively. Compared with plant fibers, GFs and EP were less hygroscopic at room temperature.

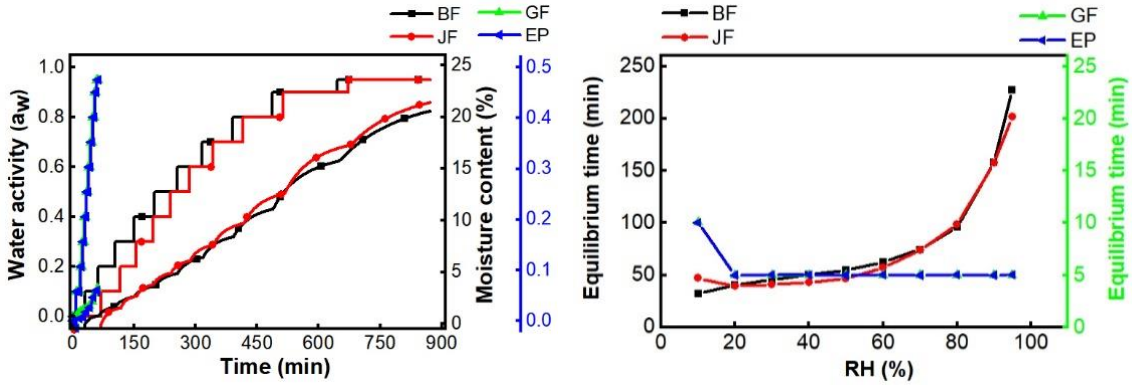

(a) Time curve of water activity and moisture content

(b) Equilibrium time - RH curve

Fig. 3. Moisture adsorption kinetic curves for different materials

The effects of water activity on BFs and JFs were greater than those on GFs and EP. The equilibrium time of BFs and JFs increased with increasing RH, and the equilibrium time of BFs was slightly longer than that of JFs. On one hand, jute is mainly built up of cellulose, which is a hydrophilic glucose polymer. The elementary unit of jute is anhydro-D-glucose, which contains three hydroxyl (-OH) groups (Zaman *et al*. 2009; Mishra *et al*. 2003). These hydroxyl groups in the cellulose structure account for the strong hydrophilic nature of jute. On the other hand, the fiber of JFs was smaller than that of BFs because of the larger surface area of JFs, which is beneficial for the sorption of the water (Yuan *et al*. 2021). This caused the EMC of JFs to be higher than that of BFs under the same RH. After the RH of GFs and EP was higher than 20%, the time required for them to reach the EMC was approximately 5 min, which was the shortest time for the experimental setup, indicating that the hygroscopic properties of the two materials was low.

Table 3. Moisture Adsorption Equilibrium Parameters for Different Materials

Index		RH (%)									
		10	20	30	40	50	60	70	80	90	95
BFs	Time (min)	62.76	103.39	149.07	199.5	254.11	316.42	390.88	486.72	644.72	872.06
	EMC (%)	0.77	1.64	2.61	3.66	4.86	6.40	8.39	11.07	15.69	20.58
JFs	Time (min)	115.72	154.98	195.74	238.53	285.3	342.33	415.92	514.45	671.58	872.86
	EMC (%)	1.51	2.65	3.76	4.88	6.07	7.62	9.69	12.56	17.23	21.42
GFs	Time (min)	17.96	22.95	27.96	32.95	37.96	42.95	47.96	52.96	57.95	62.96
	EMC (%)	0.016	0.019	0.023	0.025	0.028	0.031	0.039	0.055	0.066	0.063
EP	Time (min)	19.49	24.48	29.49	34.5	39.49	44.5	49.49	54.5	59.49	64.5
	EMC (%)	0.0045	0.0081	0.0128	0.0184	0.0245	0.031	0.0443	0.0604	0.0627	0.0508

Absorption and desorption behaviors

A comparative analysis of absorption and desorption process of the four materials is shown in Fig. 4. As shown in Fig. 4(a), the isotherms of BFs and JFs exhibited a typical sigmoidal shape (S-shape) typical, and thus it can be classified as type II according to the classification scheme of Brunauer *et al.* (1940). The adsorption isotherms of GFs and EP were similar and exhibited a typical V-shape, and they showed inflection points for adsorption at higher RH. They were characterized as microporous and mesoporous structures with limited moisture adsorption capacity and monolayer adsorption. When the RH was increasing, the EMC of BFs and JFs increased obviously compared with GFs and EP. The water vapor adsorption of BFs and JFs reached the maximum when the RH was 90%.

As shown in Fig. 4(b), BFs and JFs showed the most severe hysteresis values, followed by EP and GFs. This is because plant-derived natural fibers absorb atmospheric moisture due to the presence of hydroxyl (OH) groups associated with the cell wall macromolecules (Hill and Beck 2017), and during desorption, water loss is low. Hysteresis depends on the softening point of the material and the characteristic glass transition of the amorphous region (Salmén and Larsson 2018). The hysteresis phenomenon of BFs was

more pronounced than that of JFs when the RH was < 50%, and when the RH was > 50%, the hysteresis phenomenon of JFs were more pronounced than that of BFs, and the EMC of GFs was higher than that of EP. This is because the diameter of BFs is larger than that of JFs (Table 1), which results in a smaller surface area of BFs than JFs. There are fewer adsorption sites in BFs than JFs, so the changes in adsorption and desorption are smaller. In contrast, GFs is a monofilament fiber, and the specific surface area of GFs was much larger than that of EP, and thus, its final EMC was slightly higher than that of EP. In addition, the moisture content of the GFs returned to 0, indicating that the absorption performance of GFs was low.

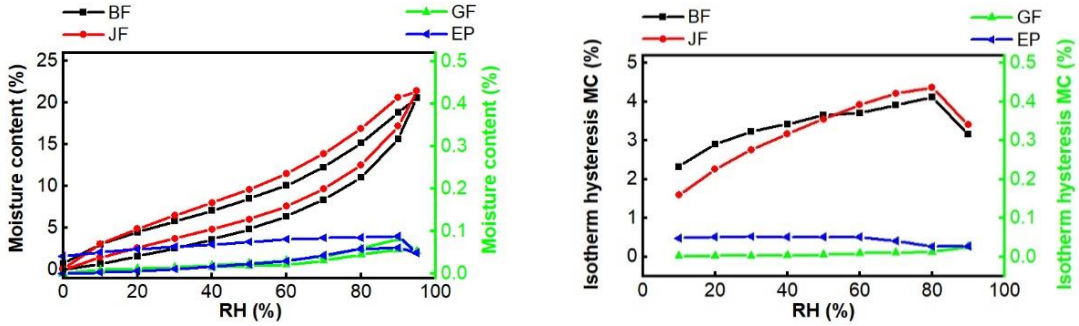

(a) Moisture absorption and desorption curve **(b)** Moisture absorption hysteresis curve

Fig. 4. Moisture absorption and desorption curves of different materials

Changes in equilibrium moisture content

The moisture content changes of the four materials during adsorption are shown in Fig. 5(a). The trends in the moisture content changes of BFs and JFs were identical to those of bamboo. The EMC of BFs and JFs was increased when the RH＜ 90% and decreased when the RH＞ 90%. The EMC of GFs and EP was increased when the RH＜ 80% and decreased when the RH＞ 80%. As shown in Fig. 5(b), when the RH was < 90%, the moisture content changes of desorption moisture content of BFs and JFs showed an increasing trend after decreasing. However, the moisture content changes of GFs and EP during desorption were not remarkable.

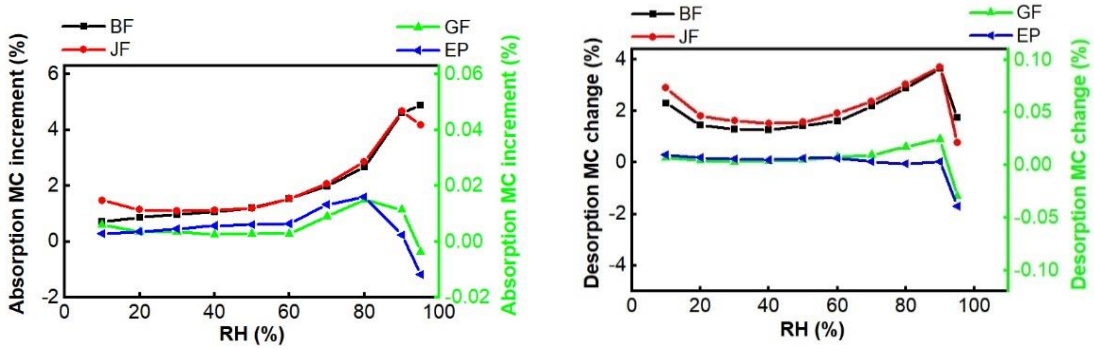

(a) Absorption moisture content value-added curve **(b)** Desorption moisture content change curve

Fig. 5. Moisture content change curve during moisture adsorption of different materials

Model fitting and evaluation of the equilibrium moisture content

The results of fitting the GAB model to the data of the EMC of four materials at different RH are shown in Table 4. The coefficients of determination R^2 were 0.999, 0.999, 0.961, and 0.917 for BFs, JFs, GFs, and EP of adsorption process, respectively. The coefficients of determination R^2 were 0.964, 0.948, 0.996, and 0.033 for desorption process, respectively, and the GAB model could not explain the desorption process of EP. The DoseResp model was used to fit the four materials. The fitting results are shown in Table 5. Using the DoseResp model for the fitting of BFs, JFs, GFs, and EP, the coefficients of determination R^2 were > 0.97 for absorption and desorption processes, indicating a good applicability of the model.

Comparative analysis of GAB and DoseResp models showed that the GAB model had better applicability in predicting the EMC of BFs and JFs, whereas the DoseResp model had better applicability in predicting the EMC of GFs and EP. Using the two models, the final EMC of BFs, JFs, GFs, and EP were 27.11%, 27.24%, 0.063%, and 0.058%, respectively.

The results of fitting the PEK model to the data of the EMC of four materials at different RH during absorption process are shown in Tables 5 and 6. As shown in Table 6, the coefficients of determination R^2 of the PEK model were > 0.999 for the four materials at different RH, and the EMC at different RH could be predicted with this model. The RH could be divided into two processes, namely, fast and slow water absorption processes, which confirmed the existence of unimolecular and multimolecular layers for water adsorption by the BFs. As shown in Table 7, the coefficient of determination R^2 of the PEK model was > 0.983 for the EP when RH was < 80%, and it decreased to 0.931 at a higher RH, indicating that the PEK model is only applicable to the hygroscopic properties of EP at low RH. The difference between the two parameters MC_1 and MC_2 was small, indicating that the moisture adsorption rate of EP was more consistent and characterized by a single molecular layer mechanism.

Table 4. GAB Model Parameters for Different Materials

Index		W_0	C	K	R_{SS}	R^2
Absorption	BFs	4.039	2.699	0.859	0.049	0.999
	JFs	4.517	4.779	0.841	0.007	0.999
	GFs	0.030	1.768	0.645	1.47E-5	0.961
	EP	2.261	0.085	0.215	4.15E-5	0.917
Desorption	BFs	4.830	4.86 E+44	0.817	1.473	0.964
	JFs	5.530	3.75E+44	0.799	2.571	0.948
	GFs	0.017	6.189	0.894	2.19E-6	0.996
	EP	0.055	7.85 E+44	0.454	2.63E-3	0.033

Table 5. DoseResp Model Parameters for Different Materials

Index		A_1	A_2	lgx_0	P	R_{SS}	R^2
Absorption	BFs	-0.154	33176.38	3.202	1.432	0.563	0.987
	JFs	-0.359	29413.67	3.563	1.204	0.653	0.986
	GFs	-0.001	0.141	1.060	1.371	1.48 E-5	0.961
	EP	0.001	0.061	0.576	3.095	2.68 E-5	0.947
Desorption	BFs	-4.693	6921.267	4.887	0.620	0.377	0.991
	JFs	-14.607	2763.858	5.892	0.381	0.464	0.991
	GFs	0.002	110.916	3.124	1.414	7.84 E-6	0.987
	EP	-0.062	0.099	-0.259	0.991	1.46 E-6	0.994

Table 6. PEK Model Parameters of BFs

RH (%)	MC_0	MC_1	t_1	MC_2	t_2	R_{SS}	R^2
10	0.032	0.553	7.976	4.693	723.412	4.98 E-06	0.999
20	0.781	0.232	5.308	0.861	30.022	6.70 E-07	0.999
30	1.667	0.194	5.533	1.007	32.378	5.29 E-07	0.999
40	2.636	0.455	9.651	1.438	97.394	2.45 E-05	0.999
50	3.665	0.130	5.352	1.322	32.852	1.84 E-06	0.999
60	4.889	0.112	5.567	1.649	32.235	1.10 E-06	0.999
70	6.409	0.208	9.572	2.084	38.323	1.45 E-06	1
80	8.412	0.380	15.563	2.715	51.852	2.00 E-06	1
90	11.052	1.494	36.948	4.055	103.153	4.60 E-06	1
95	15.669	5.007	125.159	4.145	1140.158	3.49 E-05	0.999

Table 7. PEK Model Parameters of EP

RH (%)	MC_0	MC_1	t_1	MC_2	t_2	R_{SS}	R^2
10	0.00212	0.00236	2.03631	1.57888	122642.5	6.32E-09	0.984
20	0.00473	0.00201	2.41523	0.00207	2.41536	9.03 E-09	0.991
30	0.00829	0.00335	3.78815	0.0035	3.78746	2.09 E-08	0.989
40	0.01295	0.00362	4.09917	0.00503	4.09886	2.38 E-08	0.992
50	0.0183	0.00447	3.71139	0.00463	3.71177	6.92 E-08	0.983
60	0.02469	0.00766	6.99797	0.00795	6.99893	2.94 E-08	0.993
70	0.03137	0.01364	6.2901	0.01361	6.29037	6.83 E-09	0.999
80	0.04398	-0.02351	-15.6378	-0.02433	-15.6344	1.05 E-07	0.995
90	0.0625	-0.42927	-12.4515	1.02289	-26.702	1.82 E-07	0.933
95	0.06707	-0.07313	41.54212	-0.07295	43.44859	1.63 E-06	0.931

Hygroscopic Behavior on Composites Formed by the FW of EP

Changes in moisture content and equilibrium time

The hygroscopic properties of BF-NOL, JF-NOL, and GF-NOL were determined, and the moisture adsorption kinetic curves of them were derived (Fig. 6). The EMC and the adsorption time at different RH were also analyzed (Table 8).

As shown in Fig. 6 and Table 8, the EMC of the composites increased in stages as the RH increased. However, with the increase of RH, the EMC of the BF-NOL composite reached as high as 3.35%, which was 83.7% lower than that of BFs, and the decrease was greater than that of the JF-NOL composite, which was 68.8% lower than that of BFs. This may have been because the BFs were impregnated with EP and the internal ducts and thin-walled tissues of the fibers were encapsulated by the resin, forming closed-pore structures; thus, the internal surface areas of the BF-NOL that were accessible with water molecules decreased. Additionally, the resin that penetrated the BFs was hydrophobic (Zhang *et al*. 2019), and the water adsorption sites on the surface were reduced. The EMC of the GF-NOL composite reached as high as 0.024%, but the GF-NOL was similar to GFs and EP. The effects of water activity and equilibrium time on the composites were JF-NOL, BF-NOL, and GF-NOL (in descending order), consistent with the profiles of raw materials affected by water activity. The equilibrium time required for the composites to reach the EMC was 5 min, indicating it has good water resistance.

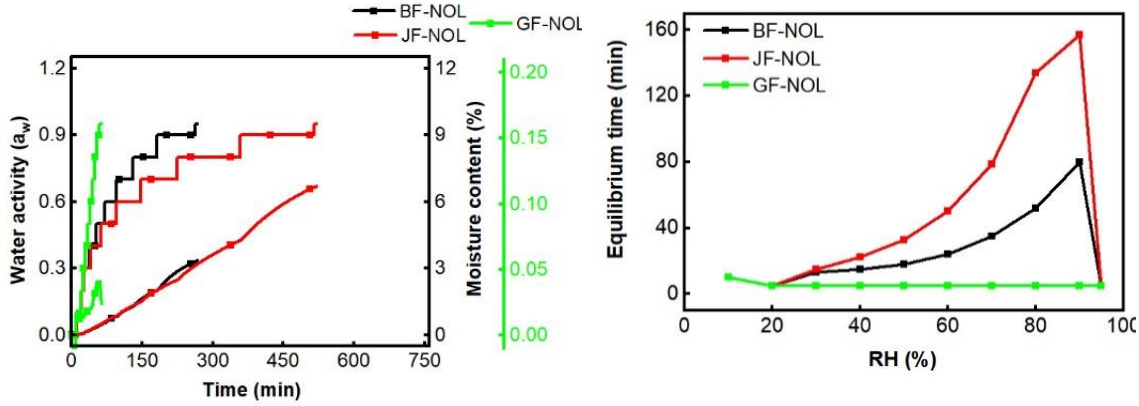

(a) Time curve of water activity and moisture content

(b) Equilibrium time - RH curve

Fig. 6. Moisture adsorption kinetic curves of circumferential composites

Table 8. Moisture Adsorption Equilibrium Parameters of Ring-Oriented Composites

Index		RH (%)									
		10	20	30	40	50	60	70	80	90	95
BF-NOL	Time (min)	19.87	24.86	38.22	53.21	71.14	95.09	129.99	182.1	262.12	267.13
	EMC (%)	0.04	0.08	0.21	0.36	0.55	0.84	1.29	2.03	3.29	3.35
JF-NOL	Time (min)	20.59	25.58	40.59	62.99	95.99	146.16	224.64	358.4	515.61	520.62
	EMC (%)	0.06	0.10	0.25	0.50	0.89	1.49	2.49	4.26	6.66	6.69
GF-NOL	Time (min)	19.14	24.13	29.14	34.13	39.13	44.14	49.14	54.14	59.14	64.13
	EMC (%)	0.013	0.014	0.016	0.019	0.021	0.024	0.032	0.040	0.039	0.024

Absorption and desorption behaviors

A comparative analysis of absorption and desorption processes of three fiber composites is shown in Fig. 7. As shown in Fig. 7(a), the adsorption isotherms of the different composites exhibited a typical V-shape. The EMC increased with the RH increasing, and because the water adsorption sites of JFs were larger than that of BFs, the EMC of the JF-NOL composites increased more than that of the BF-NOL composites. When the RH was 90%, the EMC and the water vapor adsorption of all composites reached the maximum and the composites exhibited characteristics of microporous composites.

As shown in Fig. 7(b), when the RH was between 20% and 80%, the hysteresis phenomenon of the JF-NOL composites was the most severe, followed by GF-NOL and BF-NOL. When the RH was < 20% or > 80%, the hysteresis phenomenon of the GF-NOL composites was the most severe, followed by JF-NOL and BF-NOL. Hysteresis is caused by the plastic deformation of the material (Hill *et al*. 2012). These results indicated that the dimensional change of BF-NOL was smaller at the same humidity after BFs was combined with EP.

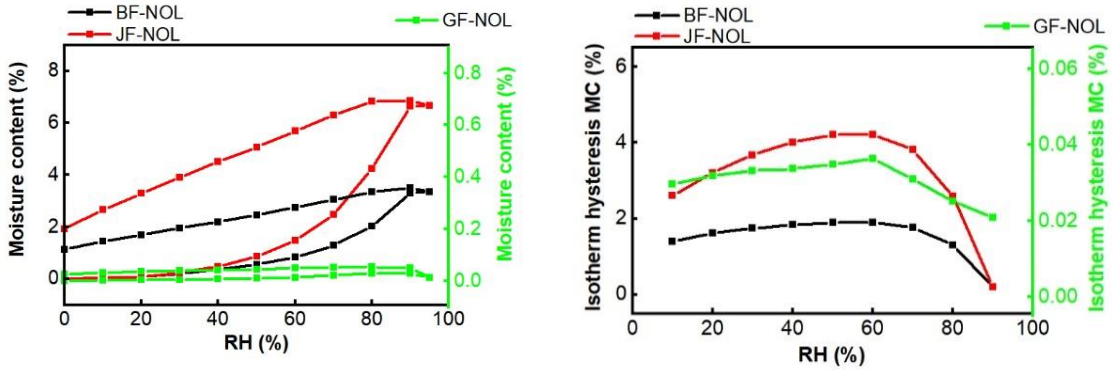

(a) Moisture absorption and desorption curve **(b)** Moisture absorption hysteresis curve

Fig. 7. Moisture absorption and desorption curves of ring-oriented composites

Changes in equilibrium moisture content

The changes of the EMC of the composites during moisture absorption and desorption were analyzed (Fig. 8). As shown in Fig. 8(a), when the RH was between 0%

and 60%, when the RH was between 70% and 90%, the EMC of the composites increased gradually the increase of the EMC of the composite was larger. When the RH was 95%, the increase of the EMC was 0, indicating that the EMC reached the maximum. As shown in Fig. 8(b), the EMC loss was relatively constant when the RH was < 80%, indicating that part of the water may have reacted with the resin and less water could be desorbed out.

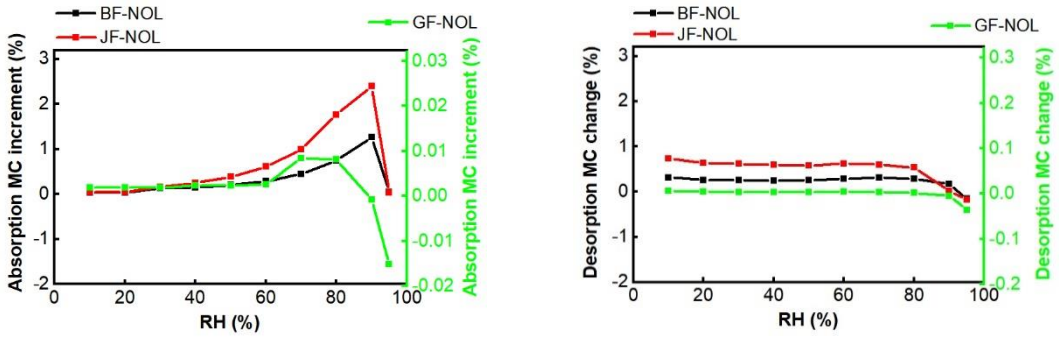

(a) Absorption moisture content value-added curve

(b) Desorption moisture content change curve

Fig. 8. Water content change curve during moisture adsorption in ring-oriented composites

Model fitting and evaluation of the equilibrium moisture content

The results of fitting the GAB model to the data of the EMC of the composites at different RH are shown in Table 9. During adsorption process, the coefficients of determination R^2 were > 0.97 for BF-NOL and JF-NOL composites, and the coefficient of determination R^2 was only 0.686 for the GF-NOL composites. During desorption, the coefficient of determination R^2 was < 0.8 for all composites, and the GAB model could not explain the adsorption and desorption processes of all composites.

The DoseResp model was selected to fit the adsorption-desorption of the composites, and the results are shown in Table 10. The coefficients of determination R^2 were > 0.95 for all composites during the absorption and desorption processes, and the model had good applicability. The EMC of the BF-NOL, JF-NOL, and GF-NOL composites reached as high as 3.946%, 7.591%, and 0.024%, respectively.

Table 9. GAB Model Parameters for Ring-Oriented Composites

Index		W_0	C	K	R_{SS}	R^2
Absorption	BF-NOL	38.214	0.024	0.646	0.030	0.981
	JF-NOL	93.966	0.017	0.664	0.199	0.970
	GF-NOL	1.705	0.388	0.037	3.30E-05	0.686
Desorption	BF-NOL	1.671	3.06E+44	0.575	0.211	0.691
	JF-NOL	3.382	2.98E+44	0.572	0.826	0.733
	GF-NOL	0.039	9.01E+44	0.086	2.50E-04	-0.603

Table 10. DoseResp Model Parameters for Ring-Oriented Composites

Index		A_1	A_2	lgx_0	P	R_{SS}	R^2
Absorption	BF-NOL	0.025	6.106	0.904	2.685	0.017	0.989
	JF-NOL	0.077	9.251	0.815	3.554	0.054	0.992
	GF-NOL	9.36E-04	0.037	0.664	2.672	4.33E-06	0.963
Desorption	BF-NOL	0.298	4.003	0.375	1.372	0.007	0.989
	JF-NOL	0.267	7.447	0.295	1.675	0.027	0.991
	GF-NOL	0.016	0.054	0.207	1.945	4.20E-06	0.953

Hygroscopic Behavior on Bamboo Fiber Composites with Different Molding Processes

Changes in moisture content and equilibrium time

The hygroscopic properties of the BF composites formed by FW, HP, and RTM moldings were determined and the moisture adsorption kinetic curves of them were derived (Fig. 9). The EMC and the adsorption time at different RH were also analyzed (Table 11).

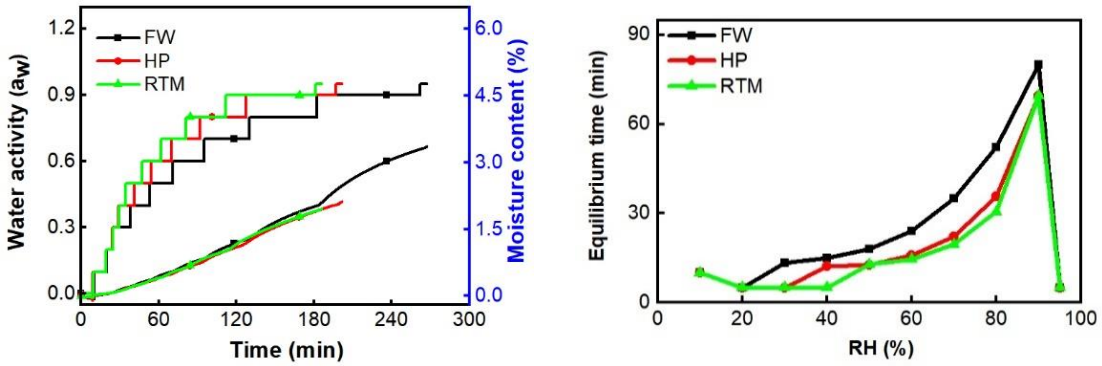

(a) Time curve of water activity and moisture (**b)** Equilibrium time - RH curve

Fig. 9. Moisture adsorption kinetic curves of different molded bamboo fiber composites

As shown in Fig. 9 and Table 11, the EMC of the composites increased in stages with the increase of the RH, and the EMC of FW, HP and RTM was 3.35%, 2.12%, and 1.96%, respectively. The effects of water activity and equilibrium time on the composites prepared by different molding processes were FW＞ HP＞ RTM molding. The equilibrium times of the three molding processes to reach the EMC were small when the RH was < 60%, and when the RH was > 70%, the equilibrium times of the three molding processes to reach the EMC were large. It rapidly decreased to 5 min when the RH was 95%.

Table 11. Moisture Adsorption Equilibrium Parameters of BF Composites

Index		Relative Humidity (%)									
		10	20	30	40	50	60	70	80	90	95
FW	Time (min)	19.87	24.86	38.22	53.21	71.14	95.09	129.99	182.1	262.12	267.13
	EMC (%)	0.04	0.08	0.21	0.36	0.55	0.84	1.29	2.04	3.29	3.35
HP	Time (min)	19.14	24.13	29.14	41.28	53.94	69.73	91.84	127.56	196.91	201.92
	EMC (%)	0.04	0.07	0.11	0.22	0.33	0.49	0.74	1.19	2.05	2.12
RTM	Time (min)	19.42	24.43	29.43	34.43	47.25	61.76	81.34	111.81	181.3	186.31
	EMC (%)	0.05	0.07	0.11	0.15	0.27	0.42	0.64	1.01	1.91	1.96

Absorption and desorption behaviors

A comparative analysis of absorption and desorption processes of BF composites prepared by different molding processes is shown in Fig. 10. The adsorption isotherms of BF composites prepared by different molding processes exhibited a typical V-shape. During absorption process, the EMC started to increase when the RH was 20% and increased rapidly when the RH was 60%, the EMC remained unchanged when the RH was > 90%. The hysteresis phenomenon was most obvious for FW composite, followed by HP and finally RTM, indicating that under external compression, the FW composite had a lower density and more defective pores, which increased the number of adsorption sites. The densification of the hollow structures in ground tissues, metaxylem vessels, and pores inside the cell lumens of bamboo during the hot-pressing process reduced the gaps and porosity in the HMP composite (Zhang *et al.* 2019).

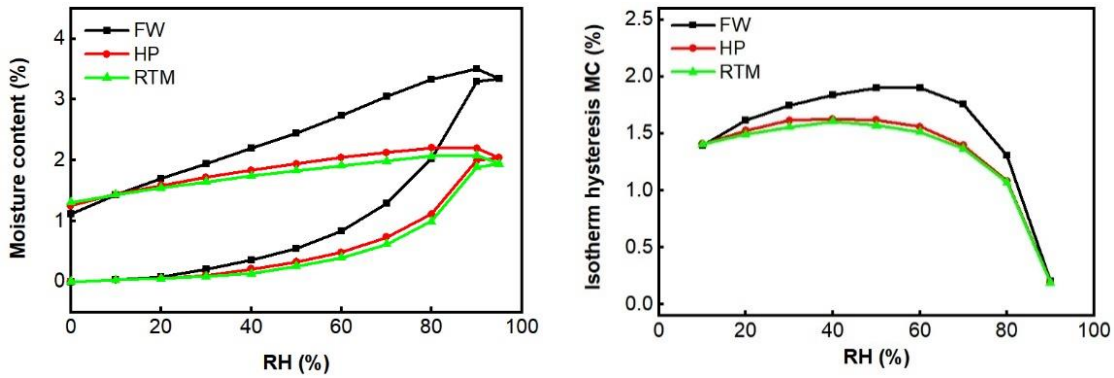

(a) Moisture absorption and desorption curve **(b)** Moisture absorption hysteresis curve

Fig. 10. Moisture absorption and desorption curves of different molded BF composites

Changes in equilibrium moisture content

The changes of the EMC of BF composites prepared by different molding processes during moisture absorption and desorption were analyzed (Fig. 11). As shown in Fig. 11(a), when the RH was between 0% and 90%, the EMC of the BF composites increased. When the RH was 95%, the change of the EMC was 0, and the surface EMC reached maximum. As shown in Fig. 11(b), the loss of the EMC of the FW composites was the largest when the RH was < 80% during desorption process.

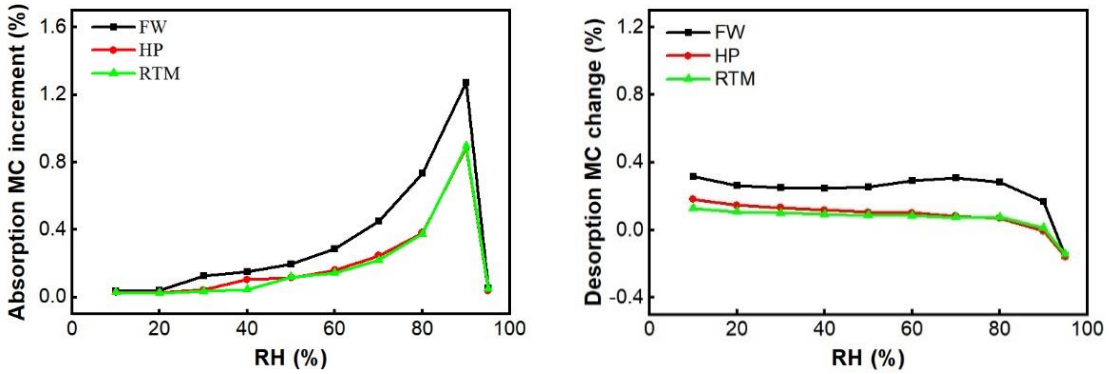

(a) Absorption moisture content value-added curve

(b) Desorption moisture content change curve

Fig. 11. Moisture adsorption water content variation curves of different molded BF composites

Model fitting and evaluation of the equilibrium moisture content

The results of fitting the GAB model to the data of the EMC of the BF composites prepared by different molding processes at different RH are shown in Table 12. During the absorption process, the coefficients of determination R^2 were > 0.975 for the BF composites prepared by different molding processes. During the desorption process, the coefficients of determination R^2 were < 0.7 for the BF composites, and the GAB model could not explain the absorption and desorption processes.

The DoseResp model was selected to fit the absorption and desorption process of BF composites prepared by different molding processes, and the relevant parameters are shown in Table 13. The coefficients of determination R^2 were > 0.96 for all composites during absorption and desorption, indicating the good applicability of the model. The EMC of the BF composites prepared by FW, HP, and RTM moldings reached as high as 3.946%, 2.474%, and 2.338%, respectively.

Table 12. GAB Model Parameters for BF Composites

Index		W_0	C	K	R_{SS}	R^2
Absorption	FW	38.214	0.024	0.646	0.03	0.981
	HP	20.519	0.023	0.669	0.012	0.979
	RTM	20.915	0.017	0.704	0.012	0.975
Desorption	FW	1.671	3.06E+44	0.575	0.211	0.691
	HP	1.557	-2.8E+44	0.324	0.212	-1.102
	RTM	1.503	5.76E+44	0.304	0.223	-2.280

Table 13. DoseResp Model Parameters for BF Composites

Index		A_1	A_2	lgx_0	P	R_{SS}	R^2
Absorption	FW	0.025	6.106	0.904	2.685	0.017	0.989
	HP	0.021	4.545	0.971	2.579	0.009	0.984
	RTM	0.039	3.552	0.913	3.180	0.008	0.983
Desorption	FW	0.298	4.003	0.375	1.372	0.007	0.989
	HP	0.921	2.184479	0.187	2.194	0.003	0.965
	RTM	1.093	2.072	0.243	2.085	0.002	0.962

CONCLUSIONS

1. The moisture adsorption isotherms of bamboo fiber (BF) and jute fiber (JF) composites conformed to type II, and the changes in adsorption and desorption processes could be predicted by the GAB model. The PEK model was used to further demonstrate the existence of unilamellar and multilamellar water adsorption modes of the BF composites, whose final equilibrium moisture content (EMC) was 27.11%. The adsorption isotherms of GFs and EP were similar and exhibited a typical V-shape, and their water content changes during desorption process could be predicted by the DoseResp model. The PEK model was used to further demonstrate the water adsorption mechanism as a single molecular layer mode, and their final EMC were 0.058% and 0.219%, respectively.
2. The moisture adsorption isotherms of BF-NOL, JF-NOL, and GF-NOL composites exhibited a typical V-shape, and their moisture content changes during adsorption and desorption processes could be predicted by the DoseResp model. Their final EMC were 3.946%, 7.591%, and 0.024%, respectively.
3. The moisture adsorption isotherms of BF composites prepared by different molding processes exhibited a typical V-shape, and their moisture content changes during adsorption and desorption processes could be predicted by the DoseResp model, which calculated the final EMC of BF composites prepared by FW, HP, and RTM moldings as 3.946%, 2.474%, and 2.338%, respectively.

ACKNOWLEDGMENTS

This work was supported by the Zhejiang Provincial Cooperative Forestry Science and Technology Project (No. 2020SY09). The constructive comments from the anonymous reviews are greatly appreciated.

REFERENCES CITED

ASTM D2291-16 (2016). "Standard practice for fabrication of ring test specimens for glass-resin composites," ASTM International, West Conshohocken, PA, USA.

Azwa, Z. N., Yousif, B. F., Manalo, A. C., and Karunasena, W. (2013). "A review on the degradability of polymeric composites based on natural fibres," *Mater. Des.* 47, 424-42. DOI: 10.1016/j.matdes.2012.11.025

Bledzki, A., and Gassan, J. (1999). "Composites reinforced with cellulose based fibres," *Polymer* 24(2), 221-274. DOI: 10.1016/s0079-6700(98)00018-5

Brunauer, S., Deming, L. S., Deming, W. E., and Teller, E. (1940). "On a theory of the van der Waals adsorption of gases," *J. Am. Chem. Soc.* 62(7), 1723-1732. DOI: 10.1021/ja01864a025

Deka, M., and Saikua, C.N. (2000). "Chemical modification of wood with thermosetting resin: Effect on dimensional stability and strength property," *Bioresour. Technol.* 73, 179-181. DOI: 10.1016/S0960-8524(99)00167-4

Hao, J. (2020). "Bamboo and hemp fiber reinforced polypropylene prepreg for winding," Doctor's Thesis, Northeast Forestry University, Harbin, China.

Hill, C., and Beck, G. (2017). "On the applicability of the Flory–Huggins and Vrentas models for describing the sorption isotherms of wood," *Int. Wood Prod. J.* 8(1), 50-55. DOI: 10.1080/20426445.2016.1275094

Hill, C. A., Keating, B. A., Jalaludin, Z., and Mahrdt, E. (2012). "A rheological description of the water vapour sorption kinetics behaviour of wood invoking a model using a canonical assembly of Kelvin-Voigt elements and a possible link with sorption hysteresis," *Holzforschung* 66, 35-47. DOI: 10.1515/hf.2011.115

Joseph, P. V., Rabello, M. S., Mattoso, L. H. C., Joseph, K., and Thomas, S. (2002). "Environmental effects on the degradation behaviour of sisal fibre reinforced polypropylene composites," *Compos Sci Technol.* 62(10), 1357-1372. DOI: 10.1016/S0266-3538(02)00080-5

Khalil, H. P. S. A., Bhat, I. U. H., Jawaid, M., Zaidon, A., Hermawan, D., and Hadi, Y. S. (2012). "Bamboo fibre reinforced biocomposites: A review," *Mater. Des.* 42, 353-368. DOI: 10.1016/j.matdes.2012.06.015

Kohler, R., Alex, R., Brielmann, R., and Ausperger, B. (2006). "A new kinetic model for water sorption isotherms of cellulosic materials," *Macromolecular Symposia* 244(1), 89-96. DOI: 10.1002/masy.200651208

Kohler, R., Dück, R., Ausperger, B., and Alex, R. (2003). "A numeric model for the kinetics of water vapor sorption on cellulosic reinforcement fibers," *Composite Interfaces* 10(2-3), 255-276. DOI: 10.1163/156855403765826900

Le, D.-G. A., Bourmaud, A., and Baley, C. (2015). "In-situ evaluation of flax fibre degradation during water ageing," *Ind Crops Prod* 70, 204-10. DOI: 10.1016/j.indcrop.2015.03.049

Li, X. (2016). "Characterization and simulation of tensile damage behavior of bamboo raw fiber reinforced composites," Master's Thesis, Southwest University, Chongqing, China.

Mishra, S., Mohanty, A. K., Drzal, L. T., Misra, M., Parija, S., Nayak, S. K., and Tripathy, S. S. (2003). "Studies on mechanical performance of biofibre/glass reinforced polyester hybrid composites," *Composite Science and Technology* 63, 1377-1385. DOI: 10.1016/S0266-3538(03)00084-8

Mittal, V., Saini, R., and Sinha, S. (2016). "Natural fiber-mediated epoxy composites–A review," Compos. 99, 425-435. DOI: 10.1016/j.compositesb.2016.06.051

Newman, R. H. (2009). "Auto-accelerative water damage in an epoxy composite reinforced with plain-weave flax fabric," *Compos A Appl Sci Manuf* 40(10),1615-1620. DOI: 10.1016/j.compositesa.2009.07.010

Peng, S., and Cai, J. (2018). "Study on the water vapor sorption properties of wood based on dvs techniques," *Journal of Anhui Agricultural University* 45(05), 877-882.

Rahman, M. R. (2018). "Influence of nanoclay/phenol formaldehyde resin on wood polymer nanocomposites," *Engineering Materials*. DOI: 10.1007/978-3-319-65735-6-8

Saba, N., Jawaid, M., Alothman, O. Y., Paridah, M., and Hassan, A. (2016). "Recent advances in epoxy resin, natural fiber-reinforced epoxy composites and their applications," *J. Reinf.* 35(6), 447-470. DOI: 10.1177/0731684415618459

Salmén, L., and Larsson, P. A. (2018). "On the origin of sorption hysteresis in cellulosic materials," *Carbohydrate polymers* 182, 15-20. DOI: 10.1016/j.carbpol.2017.11.005

Simpson, W. (1980). "Sorption theories applied to wood," *Wood Fiber* 12(3), 183-195.

Su, S. K., and Wu, C. S. (2010). "The processing and characterization of polyester/natural fiber composites," *Polym Plast Technol Eng* 49(10), 1022-1029. DOI: 10.1080/03602559.2010.482083

Sun, H., Zheng, S., Sun, M., Chen, X., and Fan Y. (2011). "Research progress of fiber reinforced epoxy composites," *Thermosetting* 26(04), 54-57. DOI: 10.1080/17415993.2010.547197

Sun, M. (2002). "Epoxy application principle and technology," China Machine Press, Beijng, China.

Tamrakar, S., and Lopez-Anido, R. A. (2011). "Water absorption of wood polypropylene composite sheet piles and its influence on mechanical properties," *Constr Build Mater* 25(10), 3977-3988. DOI: 10.1016/j.conbuildmat.2011.04.031

Wang, G., Shi, S. Q., Wang, J., Yan, Y., and Cao, S. (2011). "Tensile properties of four types of individual cellulosic fibers," *Wood Fiber Sci* 43(4), 353-364. DOI: 10.1007/s00226-010-0372-0

Xie, Y., Hill, C. A., Jalaludin, Z., Curling, S. F., Anandjiwala, R. D., Norton, A. J., and Newman, G. (2011). "The dynamic water vapour sorption behaviour of natural fibres and kinetic analysis using the parallel exponential kinetics model," *J Mater Sci* 46(2), 479-489. DOI: 10.1007/s10853-010-4935-0

Yao, Q. (2018). "Study on surface properties and moisture absorption of heat treated radiata pine," Master's Thesis, Nanjing Forestry University, Jiangsu, China.

Yao, Q., and Cai, J. (2018). "Determination and analysis of moisture adsorption and desorption isotherms of heat-treated radiata pine," *Journal of Forestry Engineering* 3(03), 35-41. DOI: 10.13360/j.issn.2096-1359.2018.03.006

Yuan, J., Chen, Q., and Fei, B. (2021). "Investigation of the water vapor sorption behavior of bamboo fibers with different sizes," *Eur. J. Wood Wood Prod.* 79(5), 1131-1139. DOI: 10.1007/s00107-020-01652-4

Zaman, H., Khan, R. A., Khan, M. A., Khan, A. H. and Hossain, M. A. (2009). "Effect of gamma radiation on the performance of jute fabrics reinforced polypropylene composites," *Radiation Physics and Chemistry* 78, 986-993. DOI: 10.1016/j.radphyschem.2009.06.011

Zelinka, S. L., Glass, S. V., and Thybring, E. E. (2018). "Myth versus reality: Do parabolic sorption isotherm models reflect actual wood–water thermodynamics?," *Wood Sci. Technol* 52(6), 1701-1706. DOI: 10.1007/s00226-018-1035-9

Zhang, X., Li, J., Yu, Y., and Wang, H. (2018). "Investigating the water vapor sorption behavior of bamboo with two sorption models," *J. Mater. Sci.* 53(11), 8241-8249. DOI: 10.1007/s10853-018-2166-y

Zhang, Y., Huang, X., Yu, Y., and Yu, W. (2019). "Effects of internal structure and chemical compositions on the hygroscopic property of bamboo fiber reinforced composites," *Appl. Surf. Sci* 492, 936-943. DOI: 10.1016/j.apsusc.2019.05.279

Article submitted: June 23, 2022; Peer review completed: August 21, 2022; Revised version received: September 15, 2022; Accepted: November 28, 2022; Published: November 9, 2022.
DOI: 10.15376/biores.18.1.272-290